Progress In Electromagnetics Research, PIER 19, 147–171, 1998

ELECTROMAGNETIC SCATTERING FROM AN INHOMOGENEOUS GRATING USING A WAVE-SPLITTING APPROACH

O. Forslund and S. He

Department of Electromagnetic Theory
Royal Institute of Technology
S-100 44 Stockholm, Sweden

1. Introduction
2. Problem Formulation and the Spectral Domain Matrix Equations
3. Vacuum Wave-Splitting for Pseudo-Periodic Fields
4. Invariant Imbedding Approach
5. Transmission Green's Function Approach
6. Numerical Examples
7. Extension to Bi-Anisotropic Gratings
8. Discussion and Conclusion
Acknowledgment
References

1. INTRODUCTION

Laterally periodic gratings have applications in many areas such as integrated optics [1], electron beams [2], holography, etc.. For the analysis of wave scattering by periodic surface gratings, or slanted gratings, there exist efficient methods such as the boundary integral method [3], the method of moment [4], and the coupled wave method [5]. However, there are much fewer efficient methods for laterally periodic gratings which are inhomogeneous in a general fashion along the vertical direction. In the present paper, we treat laterally periodic inhomogeneous gratings with a wave-splitting approach. Wave splitting means the decomposition of the total field into two components which propagate in

opposite directions. Various efficient wave-splitting approaches have been developed for scattering problems for stratified media in the frequency domain during the past years (see e.g. [6], [7]; see also [8] for wave-splitting in the time domain). Compared to other efficient numerical methods such as the finite element method [9] and the moment methods [10], the wave-splitting method gives more physical insights due to its more analytical framework.

It is well-known that scattered fields from a periodic grating are pseudo-periodic [3]. In the present paper, we generalize the plane wave vacuum-splitting [7] to the case when the electromagnetic fields are pseudo-periodic. Based on such a vacuum-splitting, both the invariant imbedding method and the transmission Green's function method are used to solve the scattering problem for a dielectric grating. The direction of incident plane wave is arbitrary and thus in general there is a cross scattering between TE and TM waves. Note that if the plane of incidence coincides with a symmetry plane, there is no cross scattering between TE and TM waves and consequently TE and TM can be treated separately. In particular, for the TE case, one only needs to consider the reduced Helmholz equation (a second order differential equation) and the analysis is given in [11]. In the present paper, an arbitrary incidence is considered and thus the treatment has to be based directly on Maxwell's equations, as a system of first order differential equations. Numerical results for the co- and cross-polarized reflection and transmission for TE and TM waves are presented. The approach is also generalized to scattering from a bi-anisotropic grating (slanted chiral gratings have been treated in [12] with a coupled wave method).

2. PROBLEM FORMULATION AND THE SPECTRAL DOMAIN MATRIX EQUATIONS

Consider an electromagnetic scattering problem for an inhomogeneous dielectric slab whose relative permittivity ε_r is laterally periodic (the permeability has a value of μ_0 everywhere). The inhomogeneous slab is confined to the region $0 \leq z \leq l$. ε_r is assumed to be $y-$ independent, and periodic in the $x-$ direction, i.e.,

$$\varepsilon_r(x+d,z) = \varepsilon_r(x,z), \qquad 0 \leq z \leq l \tag{1}$$

where $d > 0$ is the period of the permittivity. Note that the variation of ε_r in the $z-$ direction is assumed to be arbitrary. Note also that

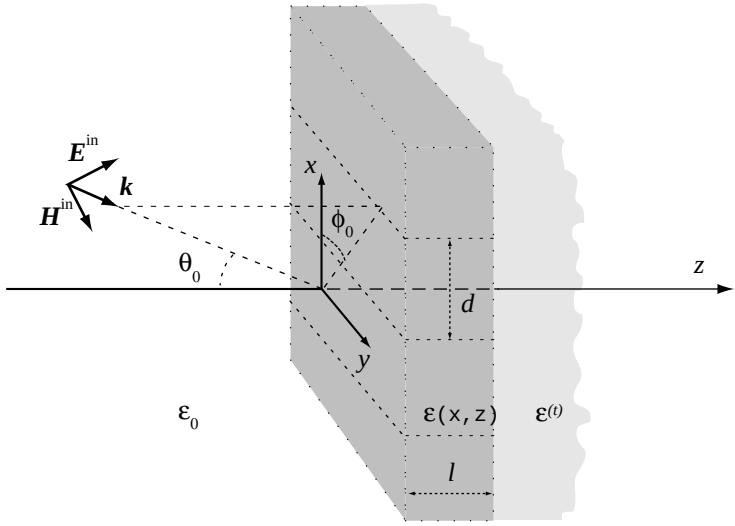

Figure 1. The scattering configuration.

ε_r may be complex so as to describe losses. There is vacuum with a permittivity ε_0 on the incidence side $z < 0$, and a homogeneous dielectric medium with a relative permittivity $\varepsilon_r^{(t)}$ on the transmission side $z > l$. The permeability is assumed to be μ_0 everywhere. A plane wave with an arbitrary polarisation (an arbitrary linear combination of TM and TE polarisations) is assumed to be incident upon the slab from a direction (θ_0, ϕ_0). The harmonic time dependence of the fields is assumed to be $\mathrm{e}^{i\omega t}$. Thus, the incident field (at $z = 0$) has the following dependence:

$$\mathrm{e}^{i(\omega t - k_{x;0}x - k_{y;0}y)},$$

where

$$k_{x;0} = k_0 \sin(\theta_0)\cos(\phi_0), \quad k_{y;0} = k_0 \sin(\theta_0)\sin(\phi_0), \tag{2}$$

and where $k_0 = \omega(\mu_0\varepsilon_0)^{1/2}$ is the wave number of the incident field. See Fig. 1 for the scattering configuration.

In the inhomogeneous slab, one has Maxwell's equations

$$\nabla \times \vec{\mathbf{E}} = -i\omega\vec{\mathbf{B}}, \qquad \nabla \times \vec{\mathbf{H}} = i\omega\vec{\mathbf{D}}, \tag{3}$$

where $\vec{\mathbf{D}} = \varepsilon_0\varepsilon_r(x,z)\vec{\mathbf{E}}$, and $\vec{\mathbf{B}} = \mu_0\vec{\mathbf{H}}$. The above Maxwell′s equations can be written in the following component form (($\hat{x}$, $\hat{y}$, $\hat{z}$) denote the unit vectors in the x, y and z directions, respectively):

$$\hat{x}:\begin{cases} \partial_z E_y = i\omega\mu_0 H_x & +\partial_y E_z, \\ \partial_z H_y = -i\omega\varepsilon_0\varepsilon_r(x,z)E_x & +\partial_y H_z, \end{cases} \tag{4}$$

$$\hat{y}:\begin{cases} \partial_z E_x = -i\omega\mu_0 H_y & +\partial_x E_z, \\ \partial_z H_x = i\omega\varepsilon_0\varepsilon_r(x,z)E_y & +\partial_x H_z, \end{cases} \tag{5}$$

$$\hat{z}:\begin{cases} H_z = -(i\omega\mu_0)^{-1} & (\partial_x E_y - \partial_y E_x), \\ E_z = (i\omega\varepsilon_0\varepsilon_r(x,z))^{-1} & (\partial_x H_y - \partial_y H_x). \end{cases} \tag{6}$$

Note that the z component of Maxwell's equations is written as Eq. (6) in such a way that the z components of the fields are expressed in terms of the tangential fields and their tangential derivatives.

The periodicity of the geometry implies that the fields are pseudo-periodic functions (i.e., $E_j(x,y,z;t)\mathrm{e}^{ik_{x;0}x}$ and $H_j(x,y,z;t)\mathrm{e}^{ik_{x;0}x}$, $j = x,y,z$, are periodic functions) in x with a period of d [3]. Thus, using the following Fourier series expansion,

$$\begin{cases} Q(x) = \sum_{n=-\infty}^{+\infty} Q_n \mathrm{e}^{-in\frac{2\pi}{d}x}, \\ Q_n = \frac{1}{d}\int_{x=-d/2}^{x=d/2} Q(x)\mathrm{e}^{in\frac{2\pi}{d}x}dx. \end{cases} \tag{7}$$

one can expand the fields as

$$\begin{cases} E_j(x,y,z;t) = \mathrm{e}^{i(\omega t - k_{x;0}x - k_{y;0}y)} \displaystyle\sum_{n=-\infty}^{+\infty} e_{j;n}(z)\ \mathrm{e}^{-in\frac{2\pi}{d}x}, \\ H_j(x,y,z;t) = \mathrm{e}^{i(\omega t - k_{x;0}x - k_{y;0}y)} \displaystyle\sum_{n=-\infty}^{+\infty} h_{j;n}(z)\ \mathrm{e}^{-in\frac{2\pi}{d}x}, \end{cases} \tag{8}$$

where $j = x,y,z$.

Using the Fourier series expansion of the fields and the orthogonality of the Fourier series, the problem is transformed into the spectral domain. The $n-$th Fourier components of Eqs. (4)–(6) give ($n = 0, \pm1, \pm2, ...$)

$$\hat{x}:\begin{cases} \partial_z e_{y;n}(z) = i\omega\mu_0 h_{x;n}(z) - ik_{y;0}e_{z;n}(z), \\ \partial_z h_{y;n}(z) = -i\omega\varepsilon_0 \displaystyle\sum_{m=-\infty}^{+\infty} (\varepsilon_r)_{n-m}e_{x;m}(z) - ik_{y;0}h_{z;n}(z), \end{cases} \tag{9}$$

$$\hat{y}: \begin{cases} \partial_z e_{x;n}(z) = -i\omega\mu_0 h_{y;n}(z) - ik_{x;n} e_{z;n}(z), \\ \partial_z h_{x;n}(z) = i\omega\varepsilon_0 \sum\limits_{m=-\infty}^{+\infty} (\varepsilon_r)_{n-m} e_{y;m}(z) - ik_{x;n} h_{z;n}(z), \end{cases} \tag{10}$$

$$\hat{z}: \begin{cases} h_{z;n}(z) = \frac{1}{\omega\mu_0}(k_{x;n} e_{y;n}(z) - k_{y;0} e_{x;n}(z)), \\ e_{z;n}(z) = \frac{1}{\omega\varepsilon_0}\Big(\sum\limits_{m=-\infty}^{+\infty} (\varepsilon_r^{-1})_{n-m}(-k_{x;m} h_{y;m}(z) + k_{y;0} h_{x;m}(z))\Big), \end{cases} \tag{11}$$

where

$$k_{x;n} = k_{x;0} + n\frac{2\pi}{d}, \tag{12}$$

and $(\varepsilon_r)_n = (\varepsilon_r)_n(z)$ and $(\varepsilon_r^{-1})_n = (\varepsilon_r^{-1})_n(z)$ denote the $n-$th Fourier coefficients of ε_r and ε_r^{-1}, respectively. Note that a multiplication of $\varepsilon_r(x,z)$ (or $(\varepsilon_r(x,z))^{-1}$) with a field becomes a discrete spatial convolution in the spectral domain. Note also that no derivatives appear in Eq. (11).

Eqs. (9)–(11) for $n = 0, \pm 1, \pm 2$, ..., give a system of infinite coupled equations. In a numerical computation, one can truncate the Fourier series by setting

$$e_{j;n} = h_{j;n} = 0, \quad j = x, y, z, \qquad \text{if } |n| \geq M, \tag{13}$$

where M is a positive integer. Thus, only a finite number of spatial harmonics are taken into account (and the higher order spatial harmonics are neglected). Such a truncation is used in the rest treatment of the paper. Denote

$$\tilde{e}_x = \begin{bmatrix} e_{x;-M} \\ \vdots \\ e_{x;M} \end{bmatrix}, \quad \tilde{e}_y = \begin{bmatrix} e_{y;-M} \\ \vdots \\ e_{y;M} \end{bmatrix}, \quad \tilde{e}_z = \begin{bmatrix} e_{z;-M} \\ \vdots \\ e_{z;M} \end{bmatrix}, \tag{14}$$

and use a similar notation for the components of the magnetic field. Furthermore let

$$\mathcal{E} = \begin{bmatrix} (\varepsilon_r)_0 & (\varepsilon_r)_{-1} & \dots & (\varepsilon_r)_{-2M} \\ (\varepsilon_r)_1 & \ddots & & \vdots \\ \vdots & & \ddots & \vdots \\ (\varepsilon_r)_{2M} & \dots & \dots & (\varepsilon_r)_0 \end{bmatrix} \tag{15}$$

$$\mathcal{F} = \begin{bmatrix} (\varepsilon_r^{-1})_0 & (\varepsilon_r^{-1})_{-1} & \cdots & (\varepsilon_r^{-1})_{-2M} \\ (\varepsilon_r^{-1})_1 & \ddots & & \vdots \\ \vdots & & \ddots & \vdots \\ (\varepsilon_r^{-1})_{2M} & \cdots & \cdots & (\varepsilon_r^{-1})_0 \end{bmatrix} \tag{16}$$

$$\mathcal{K} = \begin{bmatrix} k_{x;-M} & 0 & \cdots & 0 \\ 0 & k_{x;-M+1} & & \vdots \\ \vdots & & \ddots & 0 \\ 0 & \cdots & 0 & k_{x;M} \end{bmatrix}. \tag{17}$$

Here $\mathcal{E}$ and $\mathcal{F}$ are the convolution matrices associated with ε_r and ε_r^{-1}, respectively, and $\mathcal{K}$ is a diagonal matrix consisting of the x components of the propagation constants. We want to eliminate the z components of the fields. Truncating the Fourier expansions in Eq. (11) at $n = \pm M$, one obtains

$$\begin{bmatrix} \tilde{e}_z \\ \tilde{h}_z \end{bmatrix} = \begin{bmatrix} 0 & 0 & \frac{k_{y;0}}{\omega\varepsilon_0}\mathcal{F} & -\frac{1}{\omega\varepsilon_0}\mathcal{F}\mathcal{K} \\ -\frac{k_{y;0}}{\omega\mu_0}I & \frac{1}{\omega\mu_0}\mathcal{K} & 0 & 0 \end{bmatrix} \begin{bmatrix} \tilde{e}_x \\ \tilde{e}_y \\ \tilde{h}_x \\ \tilde{h}_y \end{bmatrix}, \tag{18}$$

where I is the identity matrix. Each submatrix has a size of $(2M+1)\times(2M+1)$. Note that $\mathcal{F}$ approaches $\mathcal{E}^{-1}$ as $M \to \infty$. If the second equation of the system (6) is multiplied by $i\omega\varepsilon_0\varepsilon_r(x,z)$ before Fourier expansion and truncation, $\mathcal{E}^{-1}$ would appear in Eq. (18) instead of $\mathcal{F}$. For a specific permittivity profile in a numerical computation, one can use $\mathcal{E}^{-1}$ as an approximation for $\mathcal{F}$, if $\mathcal{F}$ is more difficult to compute, or vice versa, use $\mathcal{F}^{-1}$ as an approximation for $\mathcal{E}$, if $\mathcal{E}$ is more difficult to compute. Denote

$$\tilde{e} = \begin{bmatrix} \tilde{e}_x \\ \tilde{e}_y \end{bmatrix}, \quad \tilde{h} = \begin{bmatrix} \tilde{h}_x \\ \tilde{h}_y \end{bmatrix}. \tag{19}$$

Truncating Eqs. (9) and (10) for $n = 0, \pm1, \pm2, ..., \pm M$, and using Eq. (18) to eliminate the z components of the fields, one obtains the following system of coupled first order differential equations in the spectral domain:

$$\partial_z \begin{bmatrix} \tilde{e} \\ \tilde{h} \end{bmatrix} \equiv \begin{bmatrix} 0 & W_b \\ W_c & 0 \end{bmatrix} \quad \begin{bmatrix} \tilde{e} \\ \tilde{h} \end{bmatrix} \equiv W \begin{bmatrix} \tilde{e} \\ \tilde{h} \end{bmatrix}, \tag{20}$$

where

$$W_b = \begin{bmatrix} -\frac{ik_{y;0}}{\omega\varepsilon_0}\mathcal{K}\mathcal{F} & -i\omega\mu_0 I + \frac{i}{\omega\varepsilon_0}\mathcal{K}\mathcal{F}\mathcal{K} \\ i\omega\mu_0 I - \frac{ik_{y;0}^2}{\omega\varepsilon_0}\mathcal{F} & \frac{ik_{y;0}}{\omega\varepsilon_0}\mathcal{F}\mathcal{K} \end{bmatrix}, \tag{21}$$

$$W_c = \begin{bmatrix} \frac{ik_{y;0}}{\omega\mu_0}\mathcal{K} & i\omega\varepsilon_0\mathcal{E} - \frac{i}{\omega\mu_0}\mathcal{K}\mathcal{K} \\ -i\omega\varepsilon_0\mathcal{E} + \frac{ik_{y;0}^2}{\omega\mu_0} I & -\frac{ik_{y;0}}{\omega\mu_0}\mathcal{K} \end{bmatrix}. \tag{22}$$

Each submatrix in the expressions (21) and (22) for W_b, W_c has a size of $(2M+1)\times(2M+1)$. Outside the inhomogeneous slab, these submatrices become simple and diagonal, and in particular $\mathcal{E}$ and $\mathcal{F}$ degenerate to I in vacuum.

3. VACUUM WAVE-SPLITTING FOR PSEUDO-PERIODIC FIELDS

In this section we decompose the tangential electric field $\tilde{e}$ into components which propagate in opposite directions, i.e, we find a transformation matrix T_0 which maps the tangential fields $\tilde{e}$ and $\tilde{h}$ into waves propagating in the forward and backward directions (with respect to the $z-$ axis) in the vacuum region. One would expect that W_0 (the matrix W in vacuum) is diagonalised in vacuum by the matrix T_0, i.e., $T_0 W_0 T_0^{-1}$ is diagonal. Furthermore, we require that each split component corresponds either to a TE or to a TM wave.

Such a splitting and diagonalisation can be performed 'mode by mode'. Each mode is associated with a propagation direction, though physically only a limited number of modes are propagating modes (with respect to z) and the rest are evanescent modes. Extracting the $n-$ th mode from the matrix W_0, one obtains the following 4×4 matrix:

$$W_{0;n} = \begin{bmatrix} 0 & 0 & -\frac{ik_{y;0}k_{x;n}}{\omega\varepsilon_0} & -i\omega\mu_0 + \frac{ik_{x;n}^2}{\omega\varepsilon_0} \\ 0 & 0 & i\omega\mu_0 - \frac{ik_{y;0}^2}{\omega\varepsilon_0} & \frac{ik_{y;0}k_{x;0}}{\omega\varepsilon_0} \\ \frac{ik_{y;0}k_{x;n}}{\omega\mu_0} & i\omega\varepsilon_0 - \frac{ik_{x;n}^2}{\omega\mu_0} & 0 & 0 \\ -i\omega\varepsilon_0 + \frac{ik_{y;0}^2}{\omega\mu_0} & -\frac{ik_{y;0}k_{x;n}}{\omega\mu_0} & 0 & 0 \end{bmatrix}. \tag{23}$$

Note that $W_{0;n}$ is not a block of W_0, but a matrix determined by $\partial_z[e_{x;n}e_{y;n}h_{x;n}h_{y;n}]^T = W_{0;n}[e_{x;n}e_{y;n}h_{x;n}h_{y;n}]^T$ in vacuum. A transformation matrix $T_{0;n}$ can then be introduced to map the tangential

mode fields $e_{x;n}$, $e_{y;n}$, $h_{x;n}$ and $h_{y;n}$ to $e^+_{1;n}$ (forward propagating TM mode), $e^+_{2;n}$ (forward propagating TE mode), $e^-_{1;n}$ (backward propagating TM mode) and $e^-_{2;n}$ (backward propagating TE mode) [13],

$$\begin{bmatrix} e^+_{1;n} \\ e^+_{2;n} \\ e^-_{1;n} \\ e^-_{2;n} \end{bmatrix} = T_{0;n} \begin{bmatrix} e_{x;n} \\ e_{y;n} \\ h_{x;n} \\ h_{y;n} \end{bmatrix}, \tag{24}$$

where

$$T_{0;n} = \frac{1}{2} \begin{bmatrix} \cos\phi_n & \sin\phi_n & -Z_{TM;n}\sin\phi_n & Z_{TM;n}\cos\phi_n \\ -\sin\phi_n & \cos\phi_n & -Z_{TE;n}\cos\phi_n & -Z_{TE;n}\sin\phi_n \\ \cos\phi_n & \sin\phi_n & Z_{TM;n}\sin\phi_n & -Z_{TM;n}\cos\phi_n \\ -\sin\phi_n & \cos\phi_n & Z_{TE;n}\cos\phi_n & Z_{TE;n}\sin\phi_n \end{bmatrix}, \tag{25}$$

$$\cos\phi_n = \frac{k_{x;n}}{(k^2_{x;n} + k^2_{y;0})^{1/2}}, \qquad \sin\phi_n = \frac{k_{y;0}}{(k^2_{x;n} + k^2_{y;0})^{1/2}}, \tag{26}$$

and where the mode impedances $Z_{TM;n}$ (for the TM mode) and $Z_{TE;n}$ (for the TE mode) are defined by

$$Z_{TM;n} = \left(-\frac{e^-_{\|n}}{h^-_{\perp n}} = \frac{e^+_{\|n}}{h^+_{\perp n}} = \right) \eta_0 \frac{k_{z,n}}{k_0} \equiv \eta_0 \cos\theta_n, \tag{27}$$

$$Z_{TE;n} = \left(\frac{e^-_{\perp n}}{h^-_{\|n}} = -\frac{e^+_{\perp n}}{h^+_{\|n}} = \right) \eta_0 \frac{k_0}{k_{z,n}} = \eta_0 / \cos\theta_n, \tag{28}$$

with $\eta_0 = (\mu_0/\varepsilon_0)^{1/2}$ and

$$k_{z;n} = \begin{cases} (k_0^2 - k^2_{x,n} - k^2_{y,0})^{1/2}, & \text{when } k^2_{x,n} + k^2_{y,0} \le k_0^2, \\ -i(k^2_{x,n} + k^2_{y,0} - k_0^2)^{1/2}, & \text{when } k^2_{x,n} + k^2_{y,0} > k_0^2 \ . \end{cases} \tag{29}$$

The matrix $T_{0;n}$ diagonalises $W_{0;n}$, i.e., $T_{0;n}W_{0;n}T^{-1}_{0;n}$ is diagonal. The eigenvalues are $\mp ik_{z;n}$. The forward and backward propagating modes are decoupled in the vacuum region. Each mode is associated with a transverse propagation direction $(k_{x;n}, k_{y;0})$, and from Eq. (42) one sees that the tangential component $e_{1;n} = e^+_{1;n} + e^-_{1;n}$ is the component parallel to this direction and the tangential component

$e_{2;n} = e^+_{2;n} + e^-_{2;n}$ perpendicular to this direction (in the direction of increasing ϕ_n). This is illustrated in Fig. 4 (associated with the second numerical example).

We can now put all the split modes together. Denote

$$\tilde{e}^+ = \begin{bmatrix} e^+_{-M} \\ \vdots \\ e^+_M \end{bmatrix}, \qquad \tilde{e}^- = \begin{bmatrix} e^-_{-M} \\ \vdots \\ e^-_M \end{bmatrix}, \tag{30}$$

where

$$e^+_n = \begin{bmatrix} e^+_{1;n} \\ e^+_{2;n} \end{bmatrix}, \qquad e^-_n = \begin{bmatrix} e^-_{1;n} \\ e^-_{2;n} \end{bmatrix}. \tag{31}$$

From Eq. (24) for $n = 0, \pm 1, \pm 2, ..., \pm M$, one obtains the following vacuum wave-splitting for the whole system

$$\begin{bmatrix} \tilde{e}^+ \\ \tilde{e}^- \end{bmatrix} = T_0 \begin{bmatrix} \tilde{e} \\ \tilde{h} \end{bmatrix}, \tag{32}$$

where

$$T_0 = \frac{1}{2} \begin{bmatrix} \Phi & \mathcal{Z}\Phi \\ \Phi & -\mathcal{Z}\Phi \end{bmatrix}, \tag{33}$$

and where Φ and $\mathcal{Z}$ are $(4M+2) \times (4M+2)$ matrices defined by

$$\Phi = [\Phi_1 \ \Phi_2], \tag{34}$$

$$\mathcal{Z} = \begin{bmatrix} Z_{-M} & 0 & \cdots & 0 \\ 0 & Z_{-M+1} & & \vdots \\ \vdots & & \ddots & 0 \\ 0 & \cdots & 0 & Z_M \end{bmatrix}, \tag{35}$$

with

$$\Phi_1 = \begin{bmatrix} \cos\phi_{-M} & 0 & \cdots \\ -\sin\phi_{-M} & 0 & \cdots \\ 0 & \ddots & 0 \\ \cdots & 0 & \cos\phi_M \\ \cdots & 0 & -\sin\phi_M \end{bmatrix}, \quad \Phi_2 = \begin{bmatrix} \sin\phi_{-M} & 0 & \cdots \\ \cos\phi_{-M} & 0 & \cdots \\ 0 & \ddots & 0 \\ \cdots & 0 & \sin\phi_M \\ \cdots & 0 & \cos\phi_M \end{bmatrix}, \tag{36}$$

$$Z_n = \begin{bmatrix} 0 & Z_{TM;n} \\ -Z_{TE;n} & 0 \end{bmatrix}. \tag{37}$$

Note that the $(4M+2)\times(2M+1)$ matrices Φ_1 and Φ_2 are (2×1) block diagonal, and the impedance matrix $\mathcal{Z}$ is (2×2) block diagonal. Consequently, one obtains the following expression for the inverse of the splitting matrix T_0,

$$T_0^{-1} = \begin{bmatrix} \Phi^{-1} & \Phi^{-1} \\ \Phi^{-1}\mathcal{Z}^{-1} & -\Phi^{-1}\mathcal{Z}^{-1} \end{bmatrix}, \tag{38}$$

where the inverses of Φ and $\mathcal{Z}$ are given by

$$\Phi^{-1} = \Phi^T, \tag{39}$$

$$\mathcal{Z}^{-1} = \begin{bmatrix} Z_{-M}^{-1} & 0 & \cdots & 0 \\ 0 & Z_{-M+1}^{-1} & & \vdots \\ \vdots & & \ddots & 0 \\ 0 & \cdots & 0 & Z_M^{-1} \end{bmatrix}. \tag{40}$$

and where the superscript T denotes the transpose, and

$$Z_n^{-1} = \begin{bmatrix} 0 & -Z_{TE;n}^{-1} \\ Z_{TM;n}^{-1} & 0 \end{bmatrix}. \tag{41}$$

Eq. (39) indicates that Φ is an orthonormal matrix.

In the present paper, we apply a vacuum wave-splitting approach to the scattering problem. A characteristic feature of a vacuum wave-splitting approach is that it is based on a wave-splitting that is not related to the media which make up the inhomogeneous structure, but is always defined with respect to vacuum. As pointed out in [7], one of the major advantages of using the vacuum wave-splitting is that the split fields are continuous across any $z-$ plane even if the parameter ε_r is discontinuous at that plane. This is because the splitting matrix T_0 is independent of any inhomogeneous parameter. Thus, substituting the vacuum wave-splitting (32) into Eq. (12), one obtains the the following system of coupled first order differential equations for the split fields,

$$\partial_z \begin{bmatrix} \tilde{e}^+ \\ \tilde{e}^- \end{bmatrix} = T_0 W T_0^{-1} \begin{bmatrix} \tilde{e}^+ \\ \tilde{e}^- \end{bmatrix} \equiv \begin{bmatrix} A & B \\ -B & -A \end{bmatrix} \begin{bmatrix} \tilde{e}^+ \\ \tilde{e}^- \end{bmatrix}, \tag{42}$$

where

$$A = \frac{1}{2}\mathcal{Z}\Phi W_c \Phi^{-1} + \frac{1}{2}\Phi W_b \Phi^{-1}\mathcal{Z}^{-1}, \tag{43}$$

$$B = \frac{1}{2}\mathcal{Z}\Phi W_c \Phi^{-1} - \frac{1}{2}\Phi W_b \Phi^{-1}\mathcal{Z}^{-1}. \tag{44}$$

$e_n^{\pm}$ only have physical meaning in vacuum as forward-going and backward-going components (TE or TM), respectively, along the diffracted direction (θ_n, ϕ_n) (defined by Eqs. (27) and (26)). There is no scattering field at angles other than these discrete diffraction angles. In particular, in the vacuum region $z < 0$,

$$e_n^+ \, \mathrm{e}^{i(\omega t - k_{x;n} x - k_{y;0} y)} = \begin{bmatrix} -\hat{z} \times \hat{z} \times \vec{\mathbf{E}}_{TM}^{inc} \\ -\hat{z} \times \hat{z} \times \vec{\mathbf{E}}_{TE}^{inc} \end{bmatrix} \delta_{n0}, \qquad z < 0 \tag{45}$$

(δ_{n0} is Kronnecker's delta function, and $-\hat{z} \times \hat{z} \times \vec{\mathbf{E}}_{TM}^{inc}$ gives the tangential TM incident electric field, etc.), and e_n^- gives the amplitudes of the reflected TM and TE wave at the diffraction direction (θ_n, ϕ_n). For large $|n|$ when $\cos\theta_n$ becomes imaginary, $e_n^{\pm}$ represent evanescent waves which propagate along a transverse direction and which are exponentially damped to zero as $|z|$ goes towards infinity. Inside the inhomogeneous grating Eq. (32) is also a useful change of basis for the spectral domain Maxwell's equations from the variables $e_{x;n}$, $e_{y;n}$, $h_{x;n}$, $h_{y;n}$ to $e_{1;n}^{\pm}$ and $e_{2;n}^{\pm}$.

4. INVARIANT IMBEDDING APPROACH

In principle one can determine the scattered fields with the invariant imbedding method. In this method one considers the imbedding geometry, i.e. a subslab $[z, l]$ of the original inhomogeneous slab $[0, l]$, and assumes that the material in the region $[0, z]$ is temporarily replaced with vacuum. For this imbedding geometry, the associated reflection coefficient matrix (denoted $\mathcal{R}(z)$) and transmission coefficient matrix (denoted by $\mathcal{T}(z)$) are defined as follows,

$$\tilde{e}^-(z) = \mathcal{R}(z)\tilde{e}^+(z), \tag{46}$$

$$\tilde{e}(l^+) = \mathcal{T}(z)\tilde{e}^+(z). \tag{47}$$

Note that $\mathcal{R}(z)$ and $\mathcal{T}(z)$ are $(4M+2) \times (4M+2)$ matrices. From the above definition one notices that $\mathcal{R}(0)$, $\mathcal{T}(0)$ are the physical reflection and transmission coefficient matrices, respectively, for the original grating.

Combining Eq. (42) with Eq. (46), one obtains the following nonlinear matrix imbedding equation (of Riccati type) for $\mathcal{R}(z)$,

$$\partial_z \mathcal{R}(z) = -B(z) - A(z)\mathcal{R}(z) - \mathcal{R}(z)A(z) - \mathcal{R}(z)B(z)\mathcal{R}(z). \tag{48}$$

The boundary value $\mathcal{R}(l^-)$ is a known matrix, i.e., the reflection coefficient matrix at an interface between vacuum and a dielectric medium with relative permittivity $\varepsilon_r^{(t)}$. If the medium on the transmission side is vacuum (i.e., $\varepsilon_r^{(t)} = 1$), one then has $\mathcal{R}(l^-) = 0$. The solution for $\mathcal{R}(z)$ is obtained by integrating Eq. (48) along the $-z$ direction starting from $z = l$.

It can be observed that $\partial_z \tilde{e}^+(l^+) = \partial_z(\mathcal{T}(z)\tilde{e}^+(z)) = 0$. If this is combined with Eqs. (42), (46) and (47), one obtains

$$\begin{cases} \partial_z \mathcal{T}(z) = & -\mathcal{T}(z)A(z) - \mathcal{T}(z)B(z)\mathcal{R}(z), \\ \mathcal{T}(l^-) & \text{is known.} \end{cases} \tag{49}$$

The boundary value $\mathcal{T}(l^-)$ is given by the transmission coefficient matrix at an interface between vacuum and a dielectric medium with relative permittivity $\varepsilon_r^{(t)}$. If the medium on the transmission side is vacuum one simply has $\mathcal{T}(l^-) = I$ (the identity matrix). Note that the above imbedding equation for transmission coefficient matrix $\mathcal{T}(z)$ is linear in $\mathcal{T}(z)$ but coupled to the reflection coefficient matrix $\mathcal{R}(z)$. The physical transmission coefficient matrix $\mathcal{T}(0)$ can be obtained by integrating the above imbedding equation along the $-z$ direction starting from $z = l$ (after $\mathcal{R}(z)$ has been computed).

The matrices $\mathcal{R}$ and $\mathcal{T}$ consist of 2×2 submatrices $\mathcal{R}_{m,n}$ and $\mathcal{T}_{m,n}$, $m, n = 0, \pm 1, \pm 2, ..., \pm M$. If $\tilde{e}_n^+(z)$ is the only present incident mode, one has

$$\tilde{e}_m^-(z) = \mathcal{R}_{m,n}(z)\,\tilde{e}_n^+(z) \equiv \begin{bmatrix} r_{1,1}^{(m,n)} & r_{1,2}^{(m,n)} \\ r_{2,1}^{(m,n)} & r_{2,2}^{(m,n)} \end{bmatrix} \tilde{e}_n^+(z), \tag{50}$$

$$\tilde{e}_m(l^+) = \mathcal{T}_{m,n}(z)\,\tilde{e}_n^+(z) \equiv \begin{bmatrix} t_{1,1}^{(m,n)} & t_{1,2}^{(m,n)} \\ t_{2,1}^{(m,n)} & t_{2,2}^{(m,n)} \end{bmatrix} \tilde{e}_n^+(z). \tag{51}$$

The coefficients of $\mathcal{R}$ relate the amplitudes of the *tangential* components of the reflected and incident electric field to each other for TM and TE modes. As is customary, the reflection coefficients for TM and TE modes which are propagating (not evanescent modes) are defined by

$$r_{XY} = \frac{E_X^s}{E_Y^{inc}}, \quad X, Y = TE \text{ or } TM, \tag{52}$$

where E_{TE}^s (E_{TE}^{inc}) is the amplitudes of the reflected (incident) electric field for TE mode, etc.. $r_{TM,TM}$, $r_{TE,TM}$ are the co- and cross-polarized reflection coefficients for TM mode incidence, respectively,

and $r_{TE,TE}$, $r_{TM,TE}$ are the co- and cross-polarized reflection coefficients for TE mode incidence, respectively. Similar definitions hold for the transmission coefficients for TM and TE modes. It is easy to see that

$$\begin{bmatrix} r_{TM,TM}^{(m,n)} & r_{TM,TE}^{(m,n)} \\ r_{TE,TM}^{(m,n)} & r_{TE,TE}^{(m,n)} \end{bmatrix} = \begin{bmatrix} r_{1,1}^{(m,n)} \frac{\cos\theta_n}{\cos\theta_m} & r_{1,2}^{(m,n)} \frac{1}{\cos\theta_m} \\ r_{2,1}^{(m,n)} \cos\theta_n & r_{2,2}^{(m,n)} \end{bmatrix}, \tag{53}$$

$$\begin{bmatrix} t_{TM,TM}^{(m,n)} & t_{TM,TE}^{(m,n)} \\ t_{TE,TM}^{(m,n)} & t_{TE,TE}^{(m,n)} \end{bmatrix} = \begin{bmatrix} t_{1,1}^{(m,n)} \frac{\cos\theta_n}{\cos\theta_m^{(t)}} & t_{1,2}^{(m,n)} \frac{1}{\cos\theta_m^{(t)}} \\ t_{2,1}^{(m,n)} \cos\theta_n & t_{2,2}^{(m,n)} \end{bmatrix}, \tag{54}$$

where

$$\cos\theta_m^{(t)} = \frac{((k^{(t)})^2 - k_{x;m}^2 - k_{y;0}^2)^{1/2}}{k^{(t)}}, \qquad k^{(t)} = \omega(\mu_0 \varepsilon_0 \varepsilon_r^{(t)})^{1/2} \tag{55}$$

($\varepsilon_r^{(t)}$ is the relative permittivity on the transmission side).

The present imbedding method seems easy to understand from a conceptional point of view. However, our numerical results and experience have shown that it is very difficult to obtain accurate numerical results by solving the nonlinear imbedding equation for the reflection coefficient matrix $\mathcal{R}$ (which is a matrix of large size) due to the nonlinear term. Thus, from a numerical point of view, the invariant imbedding method is not suitable for use for the present scattering problem. In a wave-splitting framework one may then, as an alternative consider the linear Green's functions approach [6]. In a usual Green's function approach one expresses the internal split fields in terms of the incident field. Such a Green's functions approach is not suitable for use either, since in this approach one needs to know in advance the physical reflection coefficient matrix $\mathcal{R}(0)$ [6], which is obtained by solving the nonlinear imbedding equation.

In the next section, we solve the scattering problem with a so-called transmission Green's functions approach, in which it is not required that one first solves a nonlinear equation.

5. TRANSMISSION GREEN'S FUNCTION APPROACH

In a usual Green's function approach one has to solve a system of differential equations with two boundary conditions at two endpoints

$z = 0$ and $z = l$. Such a two-endpoint-problem is difficult to solve. To overcome this difficulty, a modified Green's function approach, in which one expresses the internal split fields in terms of the transmitted field, was first introduced in the time domain [14]. As a consequence, one obtains a system of differential equations with two boundary conditions at one endpoint. Following the same idea, its frequency domain version has been used in [15]. To distinguish from the usual Green's function, we refer to such a modified Green's function as the transmission Green's function in the frequency domain (in the time domain it is referred to as the compact Green's function, since it has compact support in the time variable [14]).

Thus, define the transmission Green's function matrices $G^{\pm}(z)$ by

$$\begin{cases} \tilde{e}^{+}(z) & = G^{+}(z) \quad \tilde{e}^{+}(l^{-}), \\ \tilde{e}^{-}(z) & = G^{-}(z) \quad \tilde{e}^{+}(l^{-}). \end{cases} \tag{56}$$

where $G^{\pm}(z)$ are matrices with size $(4M+2)\times(4M+2)$. By comparing Eq. (56) with Eqs. (46) and (47), one obtains the following relations between the transmission Green's functions and the imbedding scattering coefficient matrices:

$$\begin{cases} \mathcal{R}(z) = G^{-}(z)\left[G^{+}(z)\right]^{-1}, \\ \mathcal{T}(z) = \mathcal{T}(l^{-})\left[G^{+}(z)\right]^{-1}, \end{cases} \tag{57}$$

$$\begin{cases} G^{+}(z) = \left[\mathcal{T}(z)\right]^{-1}\mathcal{T}(l^{-}), \\ G^{-}(z) = \mathcal{R}(z)\left[\mathcal{T}(z)\right]^{-1}\mathcal{T}(l^{-}). \end{cases} \tag{58}$$

Substituting the definition (56) into Eq. (42), one obtains the following system of first order linear differential equations:

$$\partial_z \begin{bmatrix} G^{+} \\ G^{-} \end{bmatrix} = \begin{bmatrix} A & B \\ -B & -A \end{bmatrix} \begin{bmatrix} G^{+} \\ G^{-} \end{bmatrix}. \tag{59}$$

The boundary conditions for the transmission Green's functions are

$$\begin{cases} G^{+}(l^{-}) = I, \\ G^{-}(l^{-}) = \mathcal{R}(l^{-}). \end{cases} \tag{60}$$

Since the split fields $\tilde{e}^{\pm}$ are continuous everywhere (as mentioned earlier), it follows from the definition (56) that the transmission Green's

functions $G^{\pm}$ are also continuous everywhere. $G^{\pm}(z)$ can be computed directly by integrating the linear system (59) along the $-z$ direction starting from $z = l$.

After the transmission Green's functions $G^{\pm}$ have been computed, the physical scattering coefficient matrices $\mathcal{R}(0)$ and $\mathcal{T}(0)$ are obtained through the relation (57) with $z = 0$.

6. NUMERICAL EXAMPLES

All the numerical results presented in this section are obtained by solving the linear system (59) and (60) for the transmission Green's functions with an explicit Runge-Kutta method.

Example 1. Consider a dielectric wedge grating superimposed on a dielectric half-space. The thickness of the grating is $l = d/2$, where the period is taken to be $d = 0.4\lambda_0$. The center dielectric wedge (with one period) has the following profile for $z \in [0, l]$ and $x \in [-d/2, d/2]$ (see the small configuration in Fig. 2(a)):

$$\varepsilon_r(x,z) = \begin{cases} \varepsilon_r(\text{constant}), \text{when} & \mid x \mid < z, \\ 1, & \text{otherwise}, \end{cases} \tag{61}$$

where $\varepsilon_r = 2 - 0.001i$. The relative permittivity of the dielectric half-space on the transmission side is $\varepsilon_r^{(t)} = 3$. The Fourier coefficients for $\varepsilon_r(x,z)$ and $\varepsilon_r^{-1}(x,z)$ for this grating are

$$(\varepsilon_r)_n(z) = \begin{cases} 1 + (\varepsilon_r - 1)\frac{2z}{d}, & n = 0, \\ \frac{1}{n\pi}(\varepsilon_r - 1)\sin(\frac{n2\pi z}{d}), & \text{otherwise}, \end{cases} \tag{62}$$

$$(\varepsilon_r^{-1})_n(z) = \begin{cases} 1 + (\varepsilon_r^{-1} - 1)\frac{2z}{d}, & n = 0, \\ \frac{1}{n\pi}(\varepsilon_r^{-1} - 1)\sin(\frac{n2\pi z}{d}), & \text{otherwise}. \end{cases} \tag{63}$$

The incident azimuthal angle ϕ_0 is fixed to be $\phi_0 = 30^\circ$. Reflection and transmission coefficient matrices have been computed for various values of the incident angle θ_0. For this example, the period d is so small that only the fundamental mode (i.e., $0-$ th mode) propagates (the rest are evanescent modes). Figs. 2(a) and 2(b) show the co- and cross-polarized reflection coefficients for the fundamental mode, respectively. Figs. 3(a) and 3(b) give the co- and cross-polarized transmission coefficients for the fundamental mode, respectively. The Fourier series

were truncated at $M = 9$ in the calculation. Note that the scattering coefficients for TE and TM modes are obtained through the relations (53) and (54) with $z = 0$. As expected, Fig. 2(b) indicates that $|r_{TE,TM}| = |r_{TM,TE}|$, which is due to the reciprocity. Note, however, reciprocity doesn't give $|t_{TE,TM}| = |t_{TM,TE}|$ since $\varepsilon_r^{(t)} \neq 1$ in this example.

Example 2. In the second numerical example, we consider a dielectric grating whose permittivity varies sinusoidally in both the vertical and lateral directions. The inhomogeneous grating has a thickness of $l = 1.2\lambda_0$ and a period of $d = 1.8\lambda_0$. On the transmission side there is vacuum. The relative permittivity has the following profile:

$$\varepsilon_r(x, z) = a + \sin(\frac{2\pi z}{l}) \cos(\frac{2\pi x}{d}), \tag{64}$$

where $a = 2.2 - 0.001i$. The Fourier coefficients for such a profile are:

$$(\varepsilon_r)_n(z) = \begin{cases} a, & n = 0\ , \\ \frac{1}{2}\sin(\frac{2\pi z}{l}), & n = \pm 1\ , \\ 0, & \text{otherwise}, \end{cases} \tag{65}$$

$$(\varepsilon_r^{-1})_n(z) = \begin{cases} a^{-1}\displaystyle\sum_{m=0}^{+\infty} (\frac{b}{a})^{2m} (\frac{1}{2})^{2m} \binom{2m}{m}, & n = 0, \\ -a^{-1}\displaystyle\sum_{m=0}^{+\infty} (\frac{b}{a})^{2m+1} (\frac{1}{2})^{2m+1} \binom{2m+1}{m-\frac{|n|-1}{2}}, & n \text{ odd}, \\ a^{-1}\displaystyle\sum_{m=0}^{+\infty} (\frac{b}{a})^{2m+2} (\frac{1}{2})^{2m+2} \binom{2m+2}{m-\frac{|n|-2}{2}}, & n \text{ even}, \end{cases} \tag{66}$$

where $b = \sin(\frac{2\pi z}{l})$. The incident angles are chosen to be $\theta_0 = 35^\circ$ and $\phi_0 = 30^\circ$. The modes are illustrated in Fig. 4. The reflection and transmission matrices have been computed, and the middle columns of $\mathcal{R}(0)$ and $\mathcal{T}(0)$ are shown below,

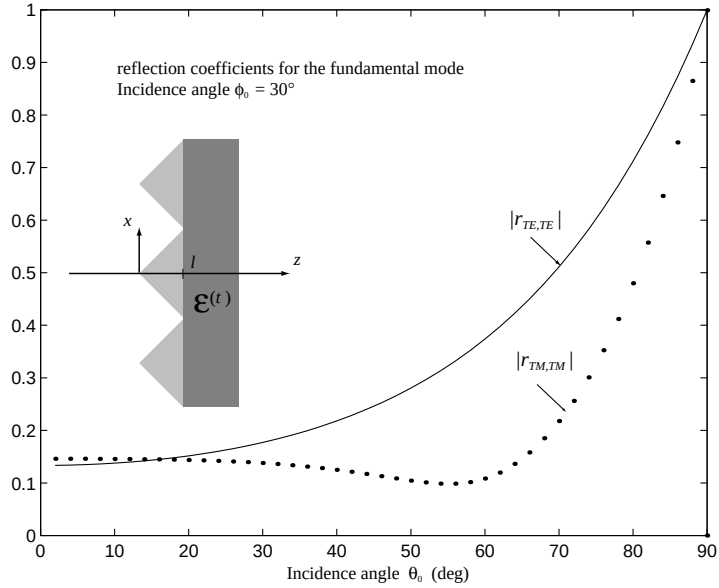

Figure 2(a) Co-polarized reflection coefficients $r^{(0,0)}_{TM,TM}$ and $r^{(0,0)}_{TE,TE}$ for the fundamental mode.

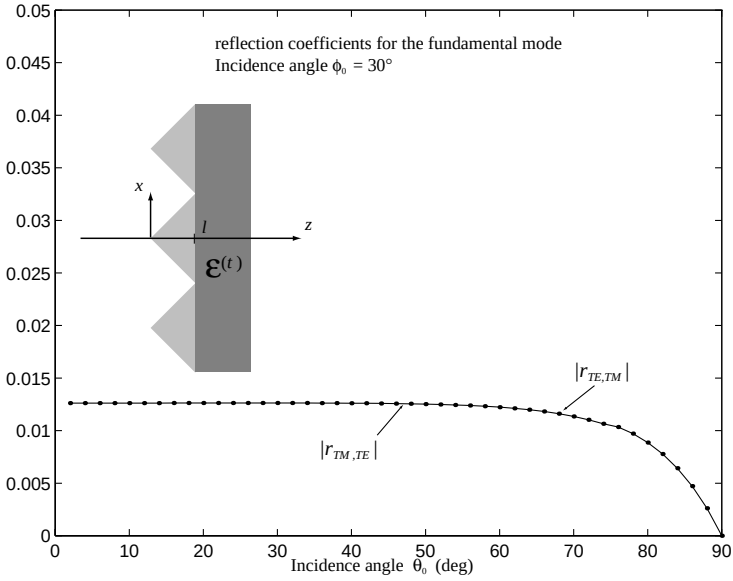

Figure 2(b) Cross-polarized reflection coefficients $r^{(0,0)}_{TM,TE}$ and $r^{(0,0)}_{TE,TM}$ for the fundamental mode.

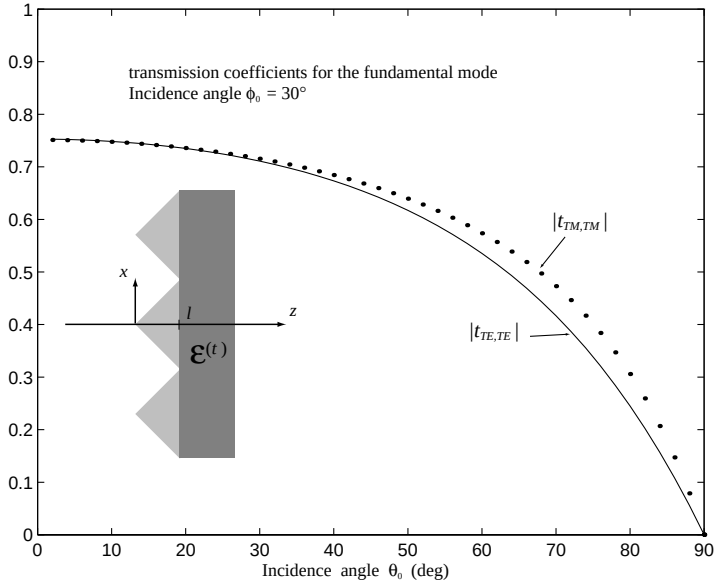

Figure 3(a) Co-polarized transmission coefficients $t^{(0,0)}_{TM,TM}$ and $t^{(0,0)}_{TE,TE}$ for the fundamental mode.

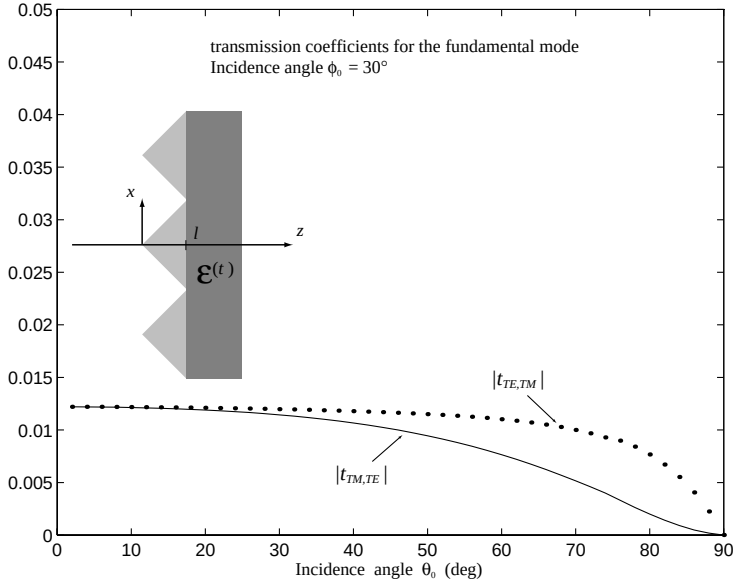

Figure 3(b) Cross-polarized transmission coefficients $t^{(0,0)}_{TM,TE}$ and $t^{(0,0)}_{TE,TM}$ for the fundamental mode.

$$\text{refl:}\begin{bmatrix}
-0.0000+0.0000i & 0.0000-0.0000i\\
0.0000-0.0000i & 0.0000-0.0000i\\
-0.0003+0.0000i & 0.0001-0.0000i\\
0.0002-0.0001i & 0.0002-0.0001i\\
-0.0046+0.0005i & 0.0016-0.0002i\\
0.0028-0.0016i & 0.0028-0.0008i\\
-0.0161+0.0009i & 0.0051+0.0003i\\
0.0258-0.0120i & 0.0251-0.0051i\\
0.0038+0.0174i & -0.0107-0.0158i\\
0.0204+0.0067i & 0.0131+0.0083i\\
0.0241+0.0053i & 0.0277-0.0115i\\
-0.0139+0.0826i & 0.0069-0.0196i\\
0.6126-0.0556i & -0.0936+0.0113i\\
-0.1395+0.0169i & -0.0428-0.0942i\\
1.3068+0.5980i & -0.2186-0.1219i\\
-0.0853+0.1054i & -0.5840+0.3475i\\
0.3490+0.1714i & -0.0641-0.0310i\\
-0.0241+0.0088i & -0.0532+0.0537i\\
0.0165+0.0095i & -0.0029-0.0016i\\
-0.0016+0.0006i & -0.0027+0.0037i\\
0.0009+0.0005i & -0.0002-0.0001i\\
-0.0001+0.0000i & -0.0001+0.0002i\\
0.0000+0.0000i & -0.0000-0.0000i\\
-0.0000+0.0000i & -0.0000+0.0000i\\
0.0000+0.0000i & -0.0000-0.0000i\\
-0.0000+0.0000i & -0.0000+0.0000i
\end{bmatrix},\quad \text{transm:}\begin{bmatrix}
0.0000+0.0000i & -0.0000-0.0000i\\
-0.0000+0.0000i & -0.0000+0.0000i\\
-0.0003-0.0001i & 0.0002+0.0000i\\
0.0002-0.0000i & 0.0001-0.0000i\\
0.0040+0.0010i & -0.0021-0.0007i\\
-0.0036+0.0007i & -0.0021+0.0001i\\
-0.0089-0.0070i & 0.0065+0.0042i\\
0.0339-0.0051i & 0.0217+0.0014i\\
0.0322-0.0300i & 0.0214+0.0124i\\
-0.0241-0.0049i & -0.0185+0.0048i\\
0.0253-0.0453i & 0.0808-0.1010i\\
-0.0502+0.0193i & 0.0178-0.0200i\\
0.0085+0.7150i & -0.1586-0.0556i\\
-0.2363-0.0828i & -0.8005+0.5062i\\
-1.5230-0.4909i & 0.2578+0.0968i\\
-0.2672-0.0378i & -0.6232+0.0401i\\
0.4354+0.1305i & -0.0673-0.0255i\\
0.0115+0.0018i & 0.0694+0.0135i\\
-0.0237-0.0060i & 0.0038+0.0010i\\
-0.0004-0.0001i & -0.0040-0.0015i\\
0.0012+0.0003i & -0.0002-0.0001i\\
-0.0000+0.0000i & 0.0001+0.0001i\\
-0.0000-0.0000i & 0.0000+0.0000i\\
0.0000-0.0000i & -0.0000-0.0000i\\
0.0000+0.0000i & -0.0000-0.0000i\\
-0.0000-0.0000i & 0.0000+0.0000i
\end{bmatrix}$$

For each of the above two matrices, the first column corresponds to the scattered TM and TE mode fields for the TM incidence, and the second column corresponds to the scattered TM and TE mode fields for the TE incidence (i.e., the first matrix consists of 2×2 matrices $\mathcal{R}_{m,0}$, $m = 0, \pm 1, \pm 2, ..., \pm M$, etc.; cf. Eqs. (50) and (51)). Modes with Fourier indices $-6, -5, \ldots, 5, 6$ were included in the calculation. Note that the absolute values of both $r_{1,1}^{(1,0)}$ and $t_{1,1}^{(1,0)}$ are larger than 1, which might seem strange. In fact this mode (with the index $n = 1$) corresponds to an evanescent wave and it does not contribute any power in the far field area. The only modes that can propagate are modes with indices $n = -2, -1, 0$. Fig. 5(a) shows the absolute values

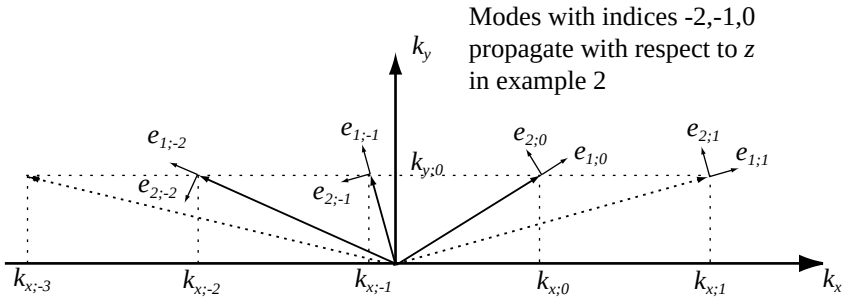

Figure 4. Propagation directions of the modes for Example 2.

of the reflected tangential fields, i.e., $|E_x^s|$ and $|E_y^s|$, on the surface $z = 0$, as functions of the lateral position x for a TE or TM incidence with unit amplitude. Fig. 5(b) gives the transmitted tangential fields $|E_x^t|$ and $|E_y^t|$ (spatial) at $z = l$. The evanescent spectral components $r_{1,1}^{(1,0)}$ and $t_{1,1}^{(1,0)}$ contribute to the near fields with large amplitudes, as can be recognized clearly in Figs. 5(a) and 5(b). These evanescent components don't contribute to the far fields but decay exponentially for large $|z|$.

7. EXTENSION TO BI-ANISOTROPIC GRATINGS

The present wave-splitting approach can be easily generalized to scattering from a bi-anisotropic grating. A bi-anisotropic medium has the following general constitutive relations

$$\vec{\mathbf{D}} = \overline{\overline{\varepsilon}}\vec{\mathbf{E}} + \overline{\overline{\xi}}\vec{\mathbf{H}}, \tag{67}$$

$$\vec{\mathbf{B}} = \overline{\overline{\mu}}\vec{\mathbf{H}} + \overline{\overline{\zeta}}\vec{\mathbf{E}}, \tag{68}$$

where $\overline{\overline{\varepsilon}}$ (the permittivity tensor), $\overline{\overline{\mu}}$ (the permeability tensor), $\overline{\overline{\xi}}$ and $\overline{\overline{\zeta}}$ are three-dimensional cartesian tensors. Assume that all the parameter tensors are $y-$ independent and periodic in the x direction with a period d, i.e.,

$$\overline{\overline{\varepsilon}}(x + d, z) = \overline{\overline{\varepsilon}}(x, z), \quad \text{etc..} \tag{69}$$

From the constitutive relations (67) and (68) and the third components of Maxwell's equations, one can always express the third components of $\vec{\mathbf{E}}$ and $\vec{\mathbf{H}}$ as linear functions of the tangential fields and

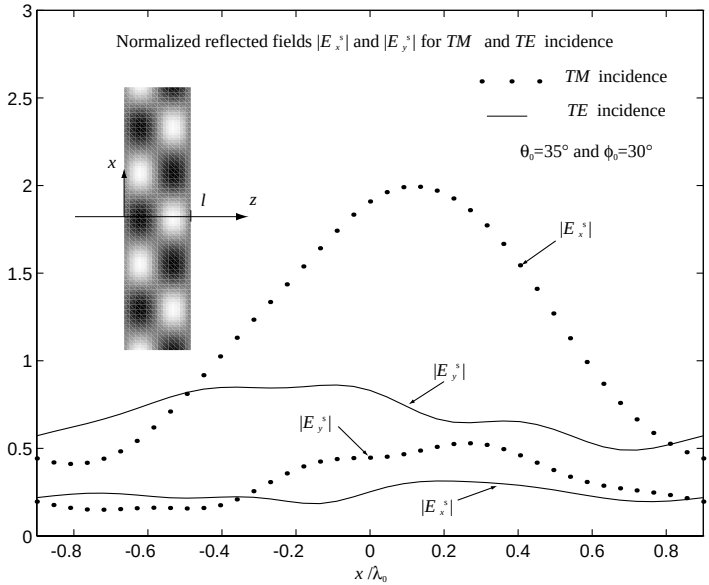

Figure 5(a) The reflected fields $|E_x^s|$ and $|E_y^s|$ at $z = 0$ for a unit TM or TE incidence.

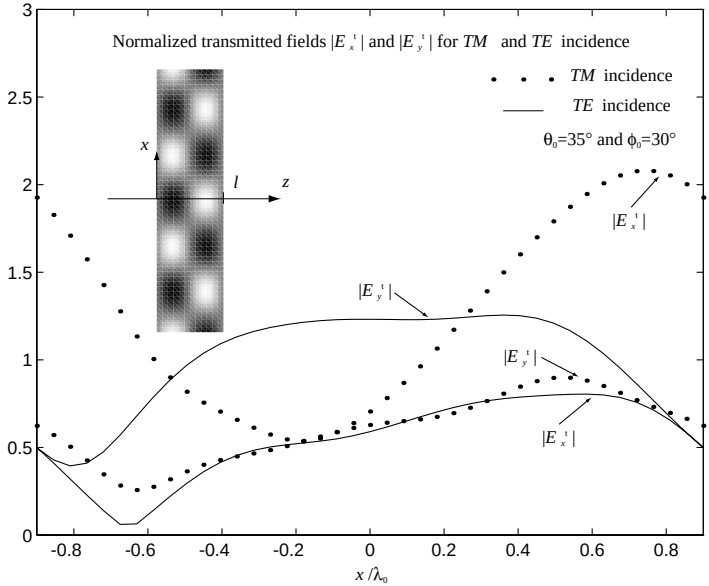

Figure 5(b) The transmitted fields $|E_x^t|$ and $|E_y^t|$ at $z = l$ for a unit TM or TE incidence.

their tangential derivatives, viz.

$$\begin{aligned} E_z =& p^{(1)}E_x + p^{(2)}E_y + p^{(3)}\partial_y E_x + p^{(4)}\partial_x E_y \\ &+ p^{(5)}H_x + p^{(6)}H_y + p^{(7)}\partial_y H_x + p^{(8)}\partial_x H_y, \end{aligned} \tag{70}$$

$$\begin{aligned} H_z =& q^{(1)}E_x + q^{(2)}E_y + q^{(3)}\partial_y E_x + q^{(4)}\partial_x E_y \\ &+ q^{(5)}H_x + q^{(6)}H_y + q^{(7)}\partial_y H_x + q^{(8)}\partial_x H_y, \end{aligned} \tag{71}$$

where $p^{(j)}$, $q^{(j)}$, $j = 1, 2, ..., 8$, are some combinations of the constitutive parameters. Since $p^{(j)}$, $q^{(j)}$ are periodic in x, and the fields have the Fourier series expansion (8), one obtains the following equations from the Fourier expansion of the above two equations,

$$\begin{aligned} e_{z;n} = \sum_{m=-\infty}^{+\infty} \{ & p^{(1)}_{n-m}e_{x;m} + p^{(2)}_{n-m}e_{y;m} - ip^{(3)}_{n-m}k_{y;0}e_{x;m} - ip^{(4)}_{n-m}k_{x;m}e_{y;m} \\ & + p^{(5)}_{n-m}h_{x;m} + p^{(6)}_{n-m}h_{y;m} - ip^{(7)}_{n-m}k_{y;0}h_{x;m} - ip^{(8)}_{n-m}k_{x;m}h_{y;m}\}, \\ h_{z;n} = \sum_{m=-\infty}^{+\infty} \{ & q^{(1)}_{n-m}e_{x;m} + q^{(2)}_{n-m}e_{y;m} - iq^{(3)}_{n-m}k_{y;0}e_{x;m} - iq^{(4)}_{n-m}k_{x;m}e_{y;m} \\ & + q^{(5)}_{n-m}h_{x;m} + q^{(6)}_{n-m}h_{y;m} - iq^{(7)}_{n-m}k_{y;0}h_{x,m} - iq^{(8)}_{n-m}k_{x;m}h_{y;m}\}, \\ & n = 0, \pm 1, \pm 2, ..., \end{aligned}$$

which can be written in the following matrix form after the truncation,

$$\begin{bmatrix} \tilde{e}_z \\ \tilde{h}_z \end{bmatrix} = P \begin{bmatrix} \tilde{e}_x \\ \tilde{e}_y \\ \tilde{h}_x \\ \tilde{h}_y \end{bmatrix}, \tag{72}$$

where P is a $2(2M+1) \times 4(2M+1)$ matrix. Using Eq. (32), one can rewrite the Fourier expansions of the first two components of Maxwell's equations in the following form

$$\partial_z \begin{bmatrix} \tilde{e} \\ \tilde{h} \end{bmatrix} = \begin{bmatrix} W_a & W_b \\ W_c & W_d \end{bmatrix} \begin{bmatrix} \tilde{e} \\ \tilde{h} \end{bmatrix}, \tag{73}$$

where W_a, W_b, W_c, and W_d are some $(2M+1)\times(2M+1)$ matrices. Applying the vacuum-splitting (32) to the above equation, one obtains

$$\partial_z \begin{bmatrix} \tilde{e}^+ \\ \tilde{e}^- \end{bmatrix} = \begin{bmatrix} A & B \\ C & D \end{bmatrix} \begin{bmatrix} \tilde{e}^+ \\ \tilde{e}^- \end{bmatrix}, \tag{74}$$

where

$$A = \frac{1}{2}\left\{\Phi W_a \Phi^{-1} + \Phi W_b \Phi^{-1} \mathcal{Z}^{-1} + \mathcal{Z}\Phi W_c \Phi^{-1} + \mathcal{Z}\Phi W_d \Phi^{-1}\mathcal{Z}^{-1}\right\},$$

$$B = \frac{1}{2}\left\{\Phi W_a \Phi^{-1} - \Phi W_b \Phi^{-1} \mathcal{Z}^{-1} + \mathcal{Z}\Phi W_c \Phi^{-1} - \mathcal{Z}\Phi W_d \Phi^{-1}\mathcal{Z}^{-1}\right\},$$

$$C = \frac{1}{2}\left\{\Phi W_a \Phi^{-1} + \Phi W_b \Phi^{-1} \mathcal{Z}^{-1} - \mathcal{Z}\Phi W_c \Phi^{-1} - \mathcal{Z}\Phi W_d \Phi^{-1}\mathcal{Z}^{-1}\right\},$$

$$D = \frac{1}{2}\left\{\Phi W_a \Phi^{-1} - \Phi W_b \Phi^{-1} \mathcal{Z}^{-1} - \mathcal{Z}\Phi W_c \Phi^{-1} + \mathcal{Z}\Phi W_d \Phi^{-1}\mathcal{Z}^{-1}\right\}.$$

Therefore, the system of differential equations for the transmission Green's functions become (cf. Eq. (59))

$$\partial_z \begin{bmatrix} G^+ \\ G^- \end{bmatrix} = \begin{bmatrix} A & B \\ C & D \end{bmatrix} \begin{bmatrix} G^+ \\ G^- \end{bmatrix}. \tag{75}$$

The boundary condition remains the same as Eq. (60). $G^{\pm}(z)$ can be computed from Eqs. (75) and (60), and the physical scattering coefficient matrices $\mathcal{R}(0)$ and $\mathcal{T}(0)$ are then obtained through the relation (57) with $z = 0$.

8. DISCUSSION AND CONCLUSION

When solving the differential equations for the transmission Green's functions by backward integration, $G^{\pm}(z)$ for the non-propagating (i.e., evanescent) modes may grow exponentially as z approaches $z = 0$. The modes with index $\pm M$ grow fastest and they may cause ill-conditioning of the matrices $G^{\pm}$ (and eventually also cause overflow) if no special care is taken. Consequently, it could become a problem to calculate accurately the inverse of $G^+(0)$ (in order to obtain $\mathcal{R}(0)$ and $\mathcal{T}(0)$; cf. Eq. (57)). Such a problem can be handled by e.g. a cascading and rescaling procedure. On the other hand, the thicker the grating is, the less these non-propagating evanescent modes (which cause some elements of $G^{\pm}$ to grow exponentially) will influence the physical scattering coefficient matrices $\mathcal{R}(0)$ and $\mathcal{T}(0)$. Therefore, the thicker the grating is, the fewer modes are required to be taken into account (i.e., using smaller integer M). In a numerical computation, the appearance of very large components in $G^{\pm}$ indicates that no more modes need to be taken into account (or should take fewer modes).

From Eqs. (28) and (27) one sees that $Z_{TE;n}$ and $Z^{-1}_{TM;n}$ are singular if $k_{z,n} = 0$ for a certain n (such a mode is called Bragg's tangent

mode). In such a case, one can compute the scattered fields by either perturbing the incident direction by a small amount (so that there is no Bragg's tangent mode), or simply remove this Bragg's tangent mode from all the matrices (technically it may be more convenient by setting all the associated elements in the matrices to zero; the amplitude of this mode can be calculated from energy conservation laws).

In the present paper, the electromagnetic scattering problem for an inhomogeneous dielectric grating has been considered. A vacuum wave-splitting for pseudo-periodic fields has been derived. The transmission Green's function approach is then used to solve the scattering problem. Numerical results for the co- and cross-polarized reflection and transmission for TE and TM incidences have been presented. Numerical results have shown that the transmission Green's function approach is superior to the invariant imbedding approach or the usual Green's function approach, for this type of scattering problem when matrices of large size are involved. The approach has also been generalized to scattering from a bi-anisotropic grating.

ACKNOWLEDGMENT

The partial support by the Swedish Research Council for Engineering Sciences and CelsiusTech Electronics AB (Sweden) is gratefully acknowledged. The authors are also grateful to Dr. Martin Norgren for valuable discussions.

REFERENCES

1. Elachi, C., and C. Yeh, "Periodic structures in integrated optics," *J. Appl. Phys.* , Vol. 44, 3146–3152, 1973.
2. Yasumoto, K., and T. Tanaka, "Radiative leakage of space-charge waves by a modulated thin-sheet electron beam propagating parallel to a reflection grating," *J. Appl. Phys.* , Vol. 62, 3543–3549, 1987.
3. Petit, R., (ed.), *Electromagnetic Theory of Gratings* , Springer-Verlag, Berlin, 1980.
4. Zaki, K. A., and A. R. Neureuther, "Scattering from a perfect conducting surface with a sinusoidal height profile: TE polarization," *IEEE Trans. Antennas Propagat.* , Vol. AP-19, 208–214, 1971.

5. Moharam, M. G., and T. K. Gaylord, "Three-dimensional vector coupled-wave analysis planar-grating diffraction," *J. Opt. Soc. Am.* , Vol. 73, No. 9, 1105–1112, 1983.
6. He, S., "A time-harmonic Green's function technique and wave propagation in a stratified nonreciprocal chiral slab with multiple discontinuities," *J. Math. Phys.* , Vol. 33, No. 12, 4103–4110, 1992.
7. Norgren, M., and S. He, "A general scheme for the electromagnetic reflection and transmission for composite structures of complex materials," *IEE Proc. Microwaves, Antennas and Propagation* , Vol. 142, No. 1, 52–56, Feb 1995.
8. He, S., S. Ström, and V. H. Weston, *Time Domian Wave-splitting and Inverse Problems* , Oxford University Press, Oxford, 1998.
9. Silvester, P. P., and R. L. Ferrari, *Finite Elements for Electrical Engineerings* , 2nd edn., Cambridge University Press, Cambridge, 1990.
10. Wang, J. J. H., *Generalized Moment Methods in Electromagnetics* , John Wiley & Sons, New York, 1991.
11. He, S., "Wave-splitting approach to a scattering problem for a laterally periodic inhomogeneous structure," *Journal of Electromagnetic Waves and Applications* , Vol. 11, 633–644, 1997
12. Yueh, S. H., and Kong, J. A., "Analysis of diffraction from chiral gratings," *Journal of Electromagnetic Waves and Applications* , Vol. 5, No. 7, 701–714, 1991.
13. Norgren, M., and S. He, "Electromagnetic reflection and transmission for a dielectric-Ω interface and a Ω slab," *International Journal of Infrared and Millimeter Waves* , Vol. 15, No. 9, 1537–1554, 1994
14. He, S., "A compact Green's function approach to the time domain direct and inverse problems for a stratified dissipative slab," *Journal of Mathematical Physics* , Vol. 34, Vo. 10, 4628–4645, 1993.
15. Norgren, M., "General optimization approach to a frequency-domain inverse problem of a stratified bi-anisotropic slab," *Journal of Electromagnetic Waves and Applications*, Vol. 11, 515–546, 1997.